# Chapter 2

# Compact Relativistic Stars under Karmarkar Condition

A class of new solutions for Einstein's field equations, by choosing the ansatz $e^{\lambda(r)} = \frac{1+k\frac{r^2}{R^2}}{1+\frac{r^2}{R^2}}$ for metric potential $g_{rr}$, are obtained under Karmarkar condition. It is found that several pulsars like 4U 1820-30, PSR J1903+327, 4U 1608-52, Vela X-1, PSR J1614-2230, Cen X-3 can be accommodated in this model. We have displayed the nature of physical parameters and energy conditions throughout the distribution using numerical and graphical methods for a particular pulsar 4U 1820-30 and found that the solution satisfies all physical requirements.

## 2.1 Introduction

Ever since Schwarzschild [169] obtained the first solution of Einstein's field equations, a plethora of exact solutions are available at present, in literature. The interest in the study of anisotropic distributions has started with theoretical investigations of Ruderman [168] and Canuto [31] regarding the anisotropic nature of matter distribution in ultra-high densities. The impact of anisotropy on an equilibrium of stellar

configuration can be seen in the pioneering work of Bowers and Liang [28]. Herrera and Santos [76] have studied matter distributions incorporating anisotropy in pressure. A class of anisotropic solutions of spherically symmetric distribution of matter has been studied by Mak and Harko [121]. Maharaj and Chaisi [123] have shown a procedure to generate anisotropic solutions from known isotropic solutions. The impact of shear and electromagnetic field on stellar configuration has been studied by Sharma and Maharaj [178].

A number of researchers have worked on spacetimes whose physical space obtained by considering t-sections has a definite geometry. Vaidya and Tikekar [211] have studied spherical distributions of matter on spacetime whose physical space has 3-spheroidal geometry. Charged analog of this metric has been studied by Patel and Koppar [153]. Tikekar and Patel [201] have obtained models of non-adiabatic gravitationally collapsing models with radial heat flux on the background of spheroidal spacetime. The impact of anisotropy on Vaidya and Tikekar [211] model has been studied by karmakar *et. al.* [87].

Tikekar and Thomas [203] have studied relativistic models of stars on the background of pseudo-spheroidal spacetime and have shown that it can be used to describe equilibrium models of superdense stars. It has further shown that these models are stable under radial modes of pulsation. Non-adiabatic gravitational collapse of spherical stars incorporating radial heat flux has been studied by Thomas and Ratanpal [197] on the background of pseudo-spheroidal spacetime. Chattopadhyay and Paul [36] have obtained the higher dimensional analog of pseudo-spheroidal stellar models of Tikekar and Thomas [204]. Ratanpal *et. al.* [158] have studied the spherical distribution of matter by choosing a specific form for radial pressure on pseudo-spheroidal spacetime. Ratanpal *et. al.* [159] have studied anisotropic models of superdense stars on the background of pseudo-spheroidal spacetime.

Another useful and geometrically significant spacetime widely used by researchers is the paraboloidal spacetime studied by Tikeker and Jotania [206]. Tikeker and Jotania [207] have used this spacetime to obtain core-envelope models of superdense stars. Anisotropic models of stars on paraboloidal spacetime admitting quadratic equation of state have been studied by Sharma and Ratanpal [179]. A new anisotropic solutions of a relativistic star on paraboloidal spacetime have been obtained by Ratanpal *et. al.* [160]. Thomas and Pandya [200] have obtained anisotropic compact star models with linear equation of state on the background of paraboloidal spacetime.

The embedding problems are geometrically significant in the general theory of relativity. Nash [138] proposed the first isometric embedding theorem. The condition for embedding 4-dimensional spacetime in 5-dimensional Euclidean space was derived by Karmarkar [86]. Such spacetimes are usually referred to as spacetimes of class I. The Karmarkar condition is given by

$$R_{1414}R_{2323} = R_{1212}R_{3434} + R_{1224}R_{1334}, \tag{2.1}$$

Pandey and Sharma [148] have found that for spherically symmetric spacetime metric to be of class-I, it is further required that $R_{2323} \neq 0$ in (2.1). Relativistic models of stars satisfying Karmarkar's condition have been extensively studied by Maurya *et. al.* ([100], [102],[103], [104], [105], [106], [112], [113]), Maurya and Govender[107], Bhar *et. al.* [16], Tello-Ortiz *et. al.* [187], Singh *et. al.* ([174], [175]).

In this article we have studied solutions of Einstein's field equations satisfying Karmarkar condition (2.1) by choosing the metric potential the ansatz $e^{\lambda(r)} = \frac{1+ar^2}{1+br^2}$. If $a = -\frac{k}{R^2}$ and $b = -\frac{1}{R^2}$, the metric in Schwarzschild coordinates represents the spheroidal spacetime metric proposed by Vaidya and Tikekar [211]. If $a = \frac{k}{R^2}$ and $b = \frac{1}{R^2}$, the spacetime metric reduces to pseudo-spheroidal spacetime metric considered by Tikekar and Thomas [203]. If we take $b = 0$ and $a = \frac{1}{R^2}$, the spacetime metric

reduces to the paraboloidal spacetime metric discussed by Tikekar and Jotania [206]. Pant *et. al.* [147] considered $a = -\frac{K}{R^2}$ and $b = -\frac{1}{R^2}$ which represents spheroidal spacetime metric and studied Vaidya-Tikekar solution under Karmarkar condition. Pandya and Thomas [150] considered $a = \frac{1}{R^2}$ and $b = 0$ that represents paraboloidal spacetime metric and studied models of compact stars on paraboloidal spacetime satisfying Karmarkar condition. We have studied compact stars on pseudo-spheroidal spacetime by considering positive values of $a$ and $b$ namely $a = \frac{K}{R^2}$ and $b = \frac{1}{R^2}$ and obtained restrictions on $a$ and $b$ using the physical acceptability conditions.

## 2.2 Einstein's Field Equations and Karmarkar Condition

We consider the interior spacetime metric for static spherically symmetric fluid distribution as

$$ds^2 = e^{\nu(r)}dt^2 - e^{\lambda(r)}dr^2 - r^2\left(d\theta^2 + \sin^2\theta d\phi^2\right), \tag{2.2}$$

with energy-momentum tensor

$$T_{ij} = (\rho + p)\, u_i u_j - p g_{ij} + \pi_{ij}, \qquad u^i u_i = 1, \tag{2.3}$$

where $\rho$ and $p$ represent density and isotropic fluid pressure respectively, $u^i$ is the unit four-velocity and anisotropic stress tensor $\pi_{ij}$ is given by Maharaj and Maartens [122]

$$\pi_{ij} = \sqrt{3}S[c_i c_j - \frac{1}{3}(u_i u_j - g_{ij})], \tag{2.4}$$

where $S = S(r)$ denotes the magnitude of anisotropy and $c^i = (0, -e^{\lambda/2}, 0, 0)$ denotes radially directed vector. The non-vanishing components of the energy-momentum

tensor are given by

$$T_0^0 = \rho, \qquad T_1^1 = -\left(p + \frac{2S}{\sqrt{3}}\right), \qquad T_2^2 = T_3^3 = -\left(p - \frac{S}{\sqrt{3}}\right). \tag{2.5}$$

We shall denote

$$p_r = p + \frac{2S}{\sqrt{3}} \qquad p_\perp = p - \frac{S}{\sqrt{3}}, \tag{2.6}$$

and hence magnitude of anisotropy is given by

$$S = \frac{p_r - p_\perp}{\sqrt{3}}. \tag{2.7}$$

The Einstein's field equations, for spacetime metric (2.2) with energy-momentum tensor (2.3), are given by

$$8\pi\rho = \frac{e^{-\lambda}\lambda'}{r} + \frac{1 - e^{-\lambda}}{r^2}, \tag{2.8}$$

$$8\pi p_r = \frac{e^{-\lambda}\nu'}{r} + \frac{e^{-\lambda} - 1}{r^2}, \tag{2.9}$$

$$8\pi p_\perp = e^{-\lambda}\left(\frac{\nu''}{2} + \frac{\nu^2}{4} - \frac{\nu'\lambda'}{4} + \frac{\nu' - \lambda'}{2r}\right). \tag{2.10}$$

The spacetime metric (2.2) is said to be of class-I type if it satisfies the Karmarkar condition (2.1). The components of Riemann curvature tensor $R_{ijkl}$ for spacetime metric (2.2) are given by

$$R_{2323} = r^2 sin^2\theta\left(1 - e^{-\lambda}\right),$$

$$R_{1212} = \frac{1}{2}r\lambda',$$

$$R_{2424} = \frac{1}{2}r\nu' e^{\nu} e^{-\lambda},$$

$$R_{1224} = 0,$$

$$R_{1414} = e^{\nu}(\frac{\nu''}{2} + \frac{\nu'^2}{4} - \frac{\lambda'\nu'}{4}),$$

$$R_{3434} = R_{2424}sin^2\theta.$$

The Karmarkar condition (2.1) now takes the form

$$\frac{\nu^{''}}{\nu^{'}} + \frac{\nu^{'}}{2} = \frac{\lambda^{'}e^{\lambda}}{2\,(e^{\lambda} - 1)}. \tag{2.11}$$

The general solution of equation (2.11) is given by

$$e^{\nu} = \left[A + B\int \sqrt{(e^{\lambda(r)} - 1)}dr\right]^2, \tag{2.12}$$

where A and B are constants of integration and $e^{\lambda(r)} \neq 1$. Using (2.9), (2.10), (2.12) in (2.7), the magnitude of anisotropy can be expressed in the form (Maurya et. al.[104])

$$8\pi\sqrt{3}S = -\frac{\nu' e^{-\lambda}}{4}\left[\frac{2}{r} - \frac{\lambda^{'}}{e^{\lambda} - 1}\right]\left[\frac{\nu' e^{\nu}}{2rB^2} - 1\right]. \tag{2.13}$$

In the case of isotropic distribution of matter, we have $S = 0$ which leads to either $\frac{2}{r} - \frac{\lambda'}{e^{\lambda}-1} = 0$ or $\frac{\nu' e^{\nu}}{2rB^2} - 1 = 0$. The former case leads to Schwarzschild [169] exterior solution and the latter gives the solution given by Kohler and Chao [92].

## 2.3 Anisotropic Solution under Karmarkar Condition

The explicit expression for the potential $\nu$ can be obtained by choosing appropriate form for $\lambda$. We choose $e^{\lambda}$ in the form

$$e^{\lambda} = \frac{1+ar^2}{1+br^2}, \tag{2.14}$$

where a and b are constants.

We shall assume here, that both $a$ and $b$ are not equal to zero. Substitution (2.14) in (2.12), gives $e^{\nu}$ in the form

$$e^{\nu} = \left(A + B\frac{\sqrt{a-b}\sqrt{1+br^2}}{b}\right)^2. \tag{2.15}$$

The spacetime metric (2.2) now takes the explicit form

$$ds^2 = \left[A + B\frac{\sqrt{a-b}\sqrt{1+br^2}}{b}\right]^2 dt^2 - \left(\frac{1+ar^2}{1+br^2}\right)dr^2 - r^2\left(d\theta^2 + \sin^2\theta d\phi^2\right). \tag{2.16}$$

The expressions of matter density, radial pressure, and tangential pressure are given by

$$8\pi\rho = \frac{(a-b)(3+ar^2)}{(1+ar^2)^2}, \tag{2.17}$$

$$8\pi p_r = \frac{Ab(b-a) + B\sqrt{a-b}\sqrt{1+br^2}(3b-a)}{(1+ar^2)(Ab + B\sqrt{a-b}\sqrt{1+br^2})}, \tag{2.18}$$

$$8\pi p_{\perp} = \frac{\sqrt{a-b}[-Ab\sqrt{a-b} + B\sqrt{1+br^2}(3b-a+abr^2)]}{(1+ar^2)^2(Ab + B\sqrt{a-b}\sqrt{1+br^2})}. \tag{2.19}$$

The hydrostatic equilibrium equation for the matter under consideration can be written as

$$\frac{dp_r}{dr} + (\rho + p_r)\left(\frac{m + 4\pi r^3 p_r}{r(r-2m)}\right) - \frac{2}{r}(p_\perp - p_r) = 0, \tag{2.20}$$

in the case of isotropic pressure distribution $(p_\perp - p_r)$, equation (2.20) takes the form of Tolman-Oppenheimer-Volkov (TOV) equation. The difference $p_\perp - p_r$ in equation (2.20) represents the force due to pressure anisotropy, which is directed inward if $p_\perp < p_r$ and outward if $p_\perp > p_r$.

The spacetime metric (2.16) should match continuously with Schwarzschild exterior metric

$$ds^2 = \left(1 - \frac{2M}{r}\right)dt^2 - \left(1 - \frac{2M}{r}\right)^{-1} dr^2 - r^2(d\theta^2 + sin^2\theta d\phi^2), \tag{2.21}$$

at the boundary of the star $r = R$. It leads to the following equations

$$1 - \frac{2M}{R} = \frac{1 + bR^2}{1 + aR^2}, \tag{2.22}$$

$$\sqrt{1 - \frac{2M}{R}} = A + B\frac{\sqrt{a-b}\sqrt{1+bR^2}}{b}. \tag{2.23}$$

Further, the boundary condition $P_r(r = R) = 0$ gives

$$Ab\sqrt{a-b} = B\sqrt{1+bR^2}\,(3b - a). \tag{2.24}$$

Equations (2.22), (2.23) and (2.24) determine the constants $A$, $B$ and the total mass enclosed inside the radius R as

$$A = \frac{(3b-a)\sqrt{1+bR^2}}{2b\sqrt{1+aR^2}}, \tag{2.25}$$

$$B = \frac{\sqrt{a-b}}{2\sqrt{1+ar^2}}, \tag{2.26}$$

$$M = \frac{(a-b)\,R^3}{2\,(1+aR^2)}. \tag{2.27}$$

Equations (2.17) through (2.19) now take the form

$$8\pi\rho = \frac{(a-b)(3+ar^2)}{(1+ar^2)^2}, \tag{2.28}$$

$$p_r = \frac{(3b-a)\,(b-a)}{1+ar^2}\left[\frac{\sqrt{1+bR^2}-\sqrt{1+br^2}}{(3b-a)\,\sqrt{1+bR^2}-(b-a)\,\sqrt{1+br^2}}\right], \tag{2.29}$$

$$p_\perp = \frac{-(a-b)[3b(1+br^2-\sqrt{1+br^2}\sqrt{1+bR^2})+a(-1+b^2r^4+\sqrt{1+br^2}\sqrt{1+bR^2})]}{(1+ar^2)^2\sqrt{1+br^2}[b(\sqrt{1+br^2}-3\sqrt{1+bR^2})+a(-\sqrt{1+br^2}+\sqrt{1+bR^2})]}. \tag{2.30}$$

The expression for anisotropy (2.13) can be explicitly written as

$$8\pi\sqrt{3}S = \frac{a(a-b)r^2[a(1+br^2-\sqrt{1+br^2}\sqrt{1+bR^2})+b(-2-2br^2+3\sqrt{1+br^2}\sqrt{1+bR^2})]}{(1+ar^2)^2\sqrt{1+br^2}[b(\sqrt{1+br^2}-3\sqrt{1+bR^2})+a(-\sqrt{1+br^2}+\sqrt{1+bR^2})]}. \tag{2.31}$$

It can be noticed that the anisotropy of the distribution is zero at the centre of the star.

## 2.4 Physical Plausibility Conditions

A physically acceptable stellar model should comply with the following conditions throughout its region of validity.

$(i)$ $\rho(r) \geq 0, \quad p_r(r) \geq 0, \quad p_\perp(r) \geq 0, \qquad \text{for } 0 \leq r \leq R$

$(ii)$ $\frac{d\rho}{dr} \leq 0, \quad \frac{dp_r}{dr} \leq 0, \quad \frac{dp_\perp}{dr} \leq 0, \qquad \text{for } 0 \leq r \leq R$

$(iii)$ $0 \leq \frac{dp_r}{d\rho} \leq 1\ , \quad 0 \leq \frac{dp_\perp}{d\rho} \leq 1, \quad \text{for } 0 \leq r \leq R$

$(iv)$ $\rho - p_r - 2p_\perp \geq 0, \qquad \text{for } 0 \leq r \leq R$

$(v)$ $\Gamma > \frac{4}{3}, \qquad \text{for } 0 \leq r \leq R$

Table 2.1: Estimated values of physical parameters based on the observational data

| **STAR** | **M** ($\mathbf{M_\odot}$) | **R** **(Km)** | $\rho_{\mathbf{c}}$ **(MeV fm$^{-3}$)** | $\rho_{\mathbf{R}}$ **(MeV fm$^{-3}$)** | $\mathbf{u}(=\frac{\mathbf{M}}{\mathbf{R}})$ |
|---|---|---|---|---|---|
| **4U 1820-30** | 1.25 | 9.1 | 804.032 | 309.128 | 0.137 |
| **PSR J1903+327** | 1.35 | 9.438 | 804.032 | 293.779 | 0.142 |
| **4U 1608-52** | 1.31 | 9.31 | 804.032 | 299.495 | 0.140 |
| **Vela X-1** | 1.38 | 9.56 | 804.032 | 288.439 | 0.144 |
| **PSR J1614-2230** | 1.42 | 9.69 | 804.032 | 282.863 | 0.146 |
| **Cen X-3** | 1.27 | 9.178 | 804.032 | 305.513 | 0.138 |

### 2.4.1 Positive Definiteness of Density and Pressure

We shall use the above conditions to find the bounds on the model parameters $a$ and $b$. Density $\rho$ is positive and decreasing throughout the distribution if $a > b$. The radial pressure $p_r$ is positive and decreasing throughout the distribution if $a \leq \frac{4}{R^2}$ and $a > 3b$, the tangential pressure $p_\perp$ is positive and decreasing throughout the distribution if $\frac{0.2749}{R^2} < a < \frac{4}{R^2}$.

### 2.4.2 Subluminal Sound Speed and Energy Conditions

The radial sound speed condition $0 < (\frac{dp_r}{d\rho})_{r=0} < 1$ impose the restrictions $0 < a \leq \frac{2.7847}{R^2}$ and $0 < (\frac{dp_r}{d\rho})_{r=R} < 1$ impose the restrictions $0 < a \leq \frac{5.4721}{R^2}$ and $a > \frac{5.4721}{R^2}$. Combining these restrictions, it shows that $0 < a \leq \frac{2.7847}{R^2}$. The tangential sound speed condition $0 < (\frac{dp_\perp}{d\rho})_{r=0} < 1$ impose the restrictions $\frac{0.4384}{R^2} < a \leq \frac{2.705}{R^2}$ and $0 < (\frac{dp_\perp}{d\rho})_{r=R} < 1$ impose the restrictions $\frac{0.2749}{R^2} < a \leq \frac{4}{R^2}, \frac{4}{R^2} < a \leq \frac{7}{R^2}, a > \frac{7}{R^2}$. combining this restrictions, It shows that $\frac{0.4384}{R^2} < a \leq \frac{2.705}{R^2}$. The strong energy condition $\rho - p_r - 2p_\perp \geq 0$ is satisfied if $0 < a \leq \frac{2}{R^2}$ and $a > b$.

### 2.4.3 Stability Criteria

The adiabatic index $\Gamma > \frac{4}{3}$ if $a \leq \frac{0.8202}{R^2}$. Thus the conditions (i) through (v) are satisfied if

$$\frac{0.4384}{R^2} < a \leq \frac{0.8202}{R^2},\ a > 3b. \tag{2.32}$$

We shall examine the viability of the present model to represent some well-known pulsars whose mass and size are known.

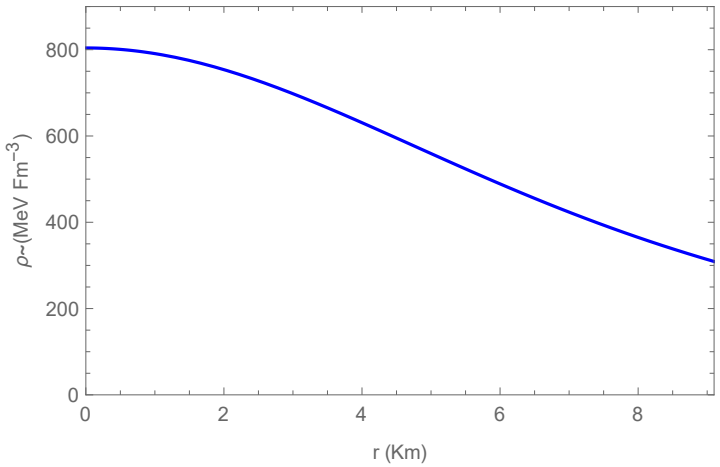


Figure 2.1: Variation of density against radial variable $r$.

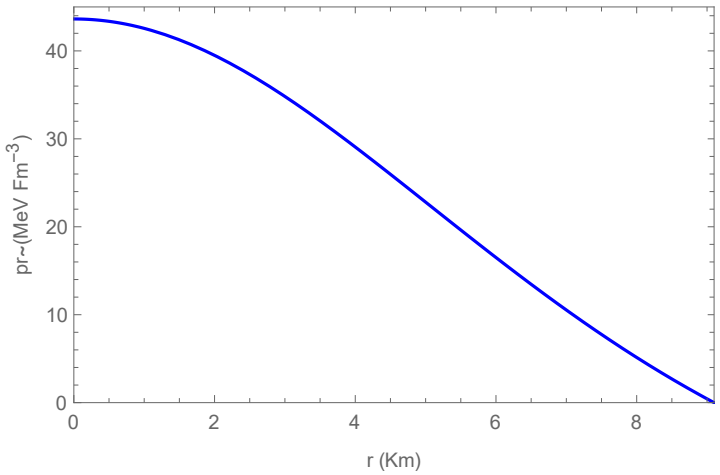


Figure 2.2: Variation of radial pressures against radial variable $r$.

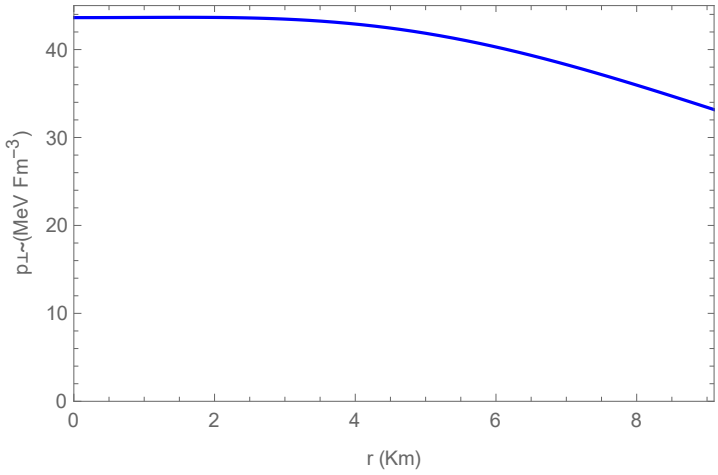


Figure 2.3: Variation of tangential pressures against radial variable $r$

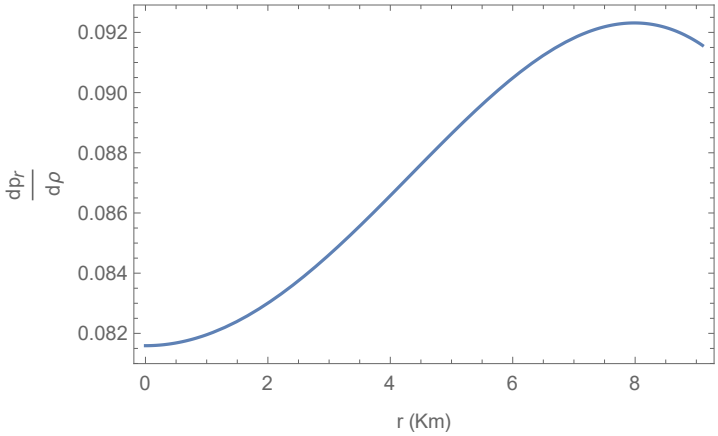


Figure 2.4: Variation of $\frac{dp_r}{d\rho}$ against radial variable $r$.

## 2.5 Discussion

We have used the present model to a large variety of compact stars like 4U 1820-30, PSR J1903+327, 4U 1608-52, Vela X-1, PSR J1614-2230, Cen X-3, whose masses and radii are known Gangopadhyay *et. al.* [61]. The central and surface densities are calculated and displayed in Table (2.1) along with the compactification factor $u$. Due to the complexity of expressions involved, it is difficult to examine the physical acceptability conditions analytically. Hence we have adopted the graphical method. In order to examine the nature of physical quantities throughout the distribution,

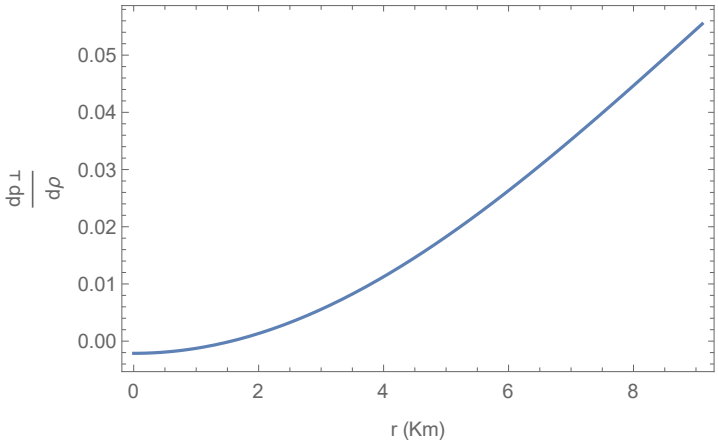


Figure 2.5: Variation of $\frac{dp_\perp}{d\rho}$ against radial variable $r$.

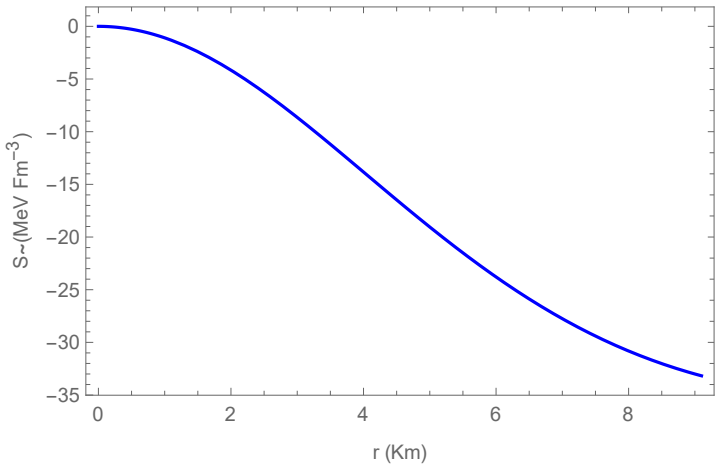


Figure 2.6: Variation of anisotropy against radial variable $r$.

we have considered the pulsar 4U 1820-30 whose estimated mass is $M = 1.25\ M_\odot$ and radius $R = 9.1\ km$. The conditions (2.32) now take the form

$$0.0053 < a \leq 0.0099,\ a > 3b. \tag{2.33}$$

We have taken the value of $a$ as the upper bound 0.0099, $b = 0.001$ and examined the physical, energy, and stability conditions of the pulsar throughout its region of validity.

In Fig. (2.1) we have shown the variation of density for $0 \leq r \leq 9.1$. It is clear from

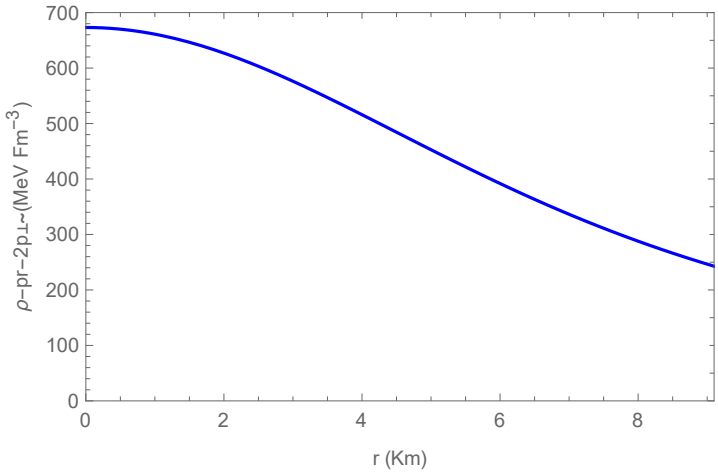


Figure 2.7: Variation of strong energy condition against radial variable $r$.

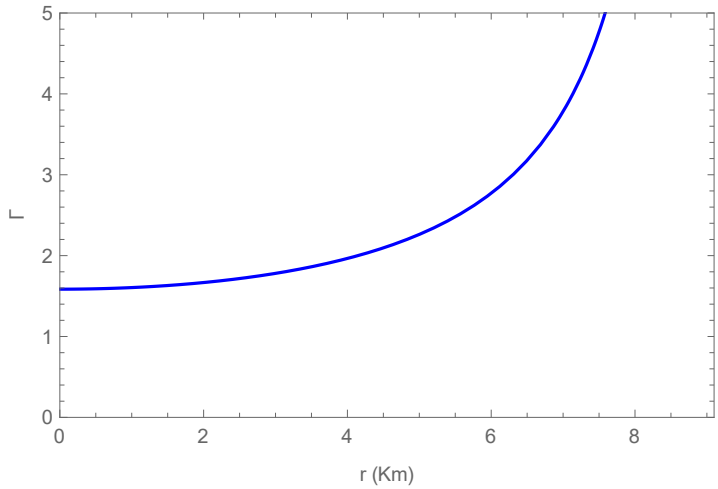


Figure 2.8: Variation of adiabatic Index against radial variable $r$.

the graph that the density is a decreasing function of $r$. In Fig.(2.2) and Fig.(2.3) we have shown the variation of radial and tangential pressure throughout the star. It can be seen that both pressures are decreasing radially outwards. In Fig.(2.4) and Fig.(2.5) we have displayed the variation of $\frac{dp_r}{d\rho}$ and $\frac{dp_\perp}{d\rho}$ against $r$. Both quantities satisfy the restriction $0 < \frac{dp_r}{d\rho} < 1$ and $0 < \frac{dp_\perp}{d\rho} < 1$ indicating that the sound speed is less than the speed of light throughout the star.

The variation of anisotropy is shown in Fig.(2.6). It can be noticed that anisotropy vanishes at the centre and decreases towards the boundary. Fig.(2.7) indicates that

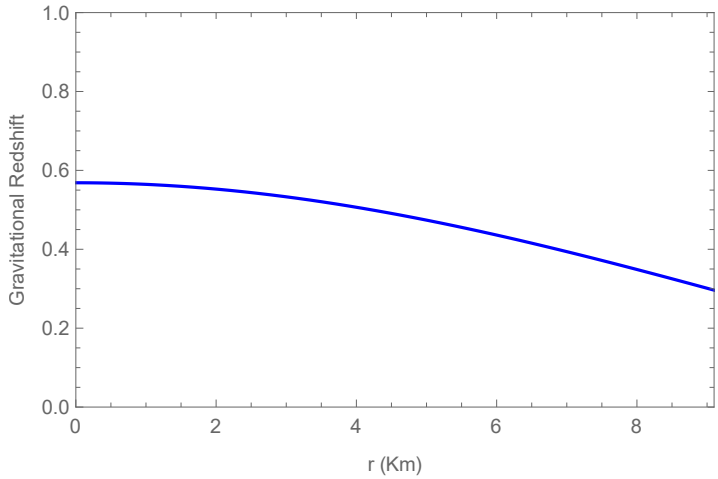


Figure 2.9: Variation of gravitational redshift against radial variable $r$.

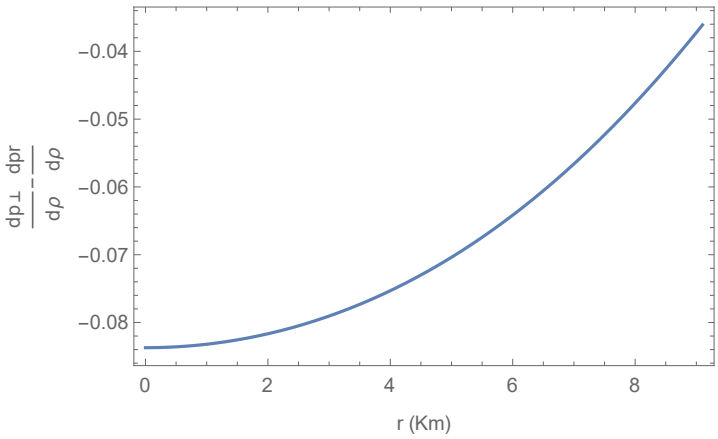


Figure 2.10: Variation of a stability expression $(\frac{dp_\perp}{d\rho} - \frac{dp_r}{d\rho})$ with respect to a radial coordinate $r$.

the strong energy condition $\rho - p_r - 2p_\perp > 0$ is satisfied througout the distribution. So that a relativistic equilibrium model of a compact star to be stable model, the adiabatic index $\Gamma = \frac{\rho+p_r}{p_r}\frac{dp_r}{d\rho} > \frac{4}{3}$ throughout the distribution. Fig.(2.8) indicates that the condition $\Gamma > \frac{4}{3}$ is satisfied in the region $0 \leq r \leq 9.1$. For a relativistic star, it is expected that the redshift must be decreasing towards the boundary and finite throughout the distribution. Fig.(2.9) shows that gravitational redshift is decreasing throughout the star under consideration. Fig.(2.10) shows that $\frac{dp_\perp}{d\rho} - \frac{dp_r}{d\rho}$ is negative throughout the star. Fig.(2.11) shows the graphical representation of

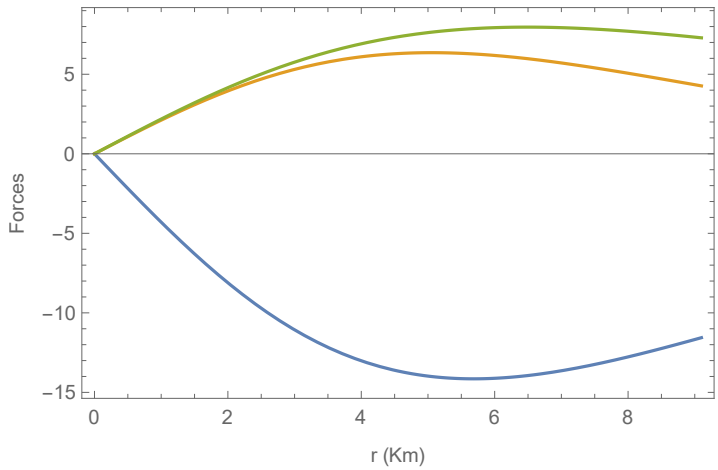


Figure 2.11: Variation of three forces like Gravitational Force(Blue), Hydrostatic Force(Orange) and Anisotropic Force(Green).

three distinct forces for the compact star 4U1820-30. According to the graphs, The gravitational force is a net negative force that predominates in nature. Hydrostatic and anisotropic forces work together to balance this force and keep the system in equilibrium.

It has been concluded that a large number of pulsars with known masses and radii can be accommodated under a model having pseudo-spheroidal geometry satisfying the Karmarkar condition.